Document Version
Final published version

Citation (APA)
Zhang, D., Pi, Z., Li, H., Xu, M., Zhou, J., Ye, G., & Zhang, M. (2025). Study on the mechanical properties of cementitious materials affected by the interactions between crystal and gel products driven by crystallization pressure. *Construction and Building Materials*, *481*, Article 141547. https://doi.org/10.1016/j.conbuildmat.2025.141547

Construction and Building Materials 481 (2025) 141547

Contents lists available at ScienceDirect

Construction and Building Materials

journal homepage: www.elsevier.com/locate/conbuildmat

Study on the mechanical properties of cementitious materials affected by the interactions between crystal and gel products driven by crystallization pressure

Depeng Zhang [a], Zhenyu Pi [a], Hui Li [a], Mingfeng Xu [a], Jian Zhou [a,*], Guang Ye [b], Mingzhong Zhang [c]

[a] School of Civil and Transportation Engineering, Hebei University of Technology, Tianjin 300401, China
[b] Department of Materials and Environment (Microlab), Faculty of Civil Engineering and Geoscience, Delft University of Technology, Delft 2628 CN, Netherlands
[c] Department of Civil, Environmental and Geomatic Engineering, University College London, London WC1E 6BT, UK

ARTICLE INFO

Keywords:
Moisture content
Crystallization pressure
Solution exchange
Mechanical properties
Cementitious materials

ABSTRACT

Existing research on the mechanisms affecting the strength of cementitious materials primarily focuses on the composition and properties of cement hydration products, often overlooking the interactions between different products. This study presents a systematic experimental and theoretical investigation into the mechanical properties of cementitious materials, emphasizing the interactions between crystal and gel products driven by crystallization pressure. A new mechanism based on crystallization pressure is proposed to explain the impact of the interactions between hydration products on the strengths of cementitious materials. Experiments were conducted by immersing specimens in solutions with tailored ion concentrations (including water, isopropyl alcohol, ethanol, and solutions of calcium hydroxide and calcium acetate) to vary the crystallization pressure. The flexural and compressive strengths of these specimens were then tested. An analytical model was developed and validated against the experimental data. Both experimental and calculated results demonstrate a negative correlation between crystallization pressure and strength. Specimens subjected to crystallization pressures of 101.7 MPa and 147.8 MPa showed reductions in flexural strength of 19.34 % and 30.65 %, respectively, and decreases in compressive strength of 10.00 % and 14.41 %, compared to control specimens with zero crystallization pressure. These results suggest that ion concentrations in the pore solution alter the crystallization pressure, which in turn affects the interactions between crystal and gel products and strength of cementitious materials. This study provides insights into the mechanisms of strength degradation due to moisture in porous materials.

1. Introduction

The strength of cementitious materials is widely regarded as their most critical property, primarily determined by the hydration products of cement [1]. The main compounds in cement undergo hydration reactions in the presence of water. For Portland cement, the hydration reactions produce calcium silicate hydrate (C-S-H) and calcium hydroxide (CH). These products are essential for the mechanical properties of the cementitious material [2–4]. The development of strength in hydrated cement paste is governed by the continued formation and growth of hydration products [5]. In the early stage of hydration, the C-S-H in the hydration products forms a dense network structure [6,7], while CH crystals grow within this network to fill the spaces [8], leading to a denser cement paste with a continuous reduction in porosity. During this period, the strength of the cement paste increases rapidly. As hydration progresses, the rate of hydration product formation diminishes, and the increase in cement paste strength decelerates, ultimately resulting in a stronger material. Thus, hydration products play a critical role in the strength development of cement paste [9].

In existing studies on the mechanical properties of cementitious materials, hydration products are generally treated as a single entity [10–12]. However, studies have shown that the main hydration products of Portland cement, C-S-H and CH, exhibit distinct properties. In the X-ray diffraction (XRD) patterns of cement paste, CH exhibits a strong diffraction peak, indicating high crystallinity, while C-S-H exhibits a

---

* Corresponding author.
E-mail address: zhoujian@hebut.edu.cn (J. Zhou).

https://doi.org/10.1016/j.conbuildmat.2025.141547
Received 5 March 2025; Received in revised form 15 April 2025; Accepted 27 April 2025

List of symbols

E	Elastic modulus of cement paste
E_{cry}	Elastic modulus of the crystal phase
E_{gel}	Elastic modulus of the gel phase
E_p	Elastic modulus of the pore phase
K	Parameter related to the E, E_p, $R_{c/g}$, and ϕ
K^{ion}	Equilibrium solubility
P	External stress
P_{11}	Tensile strength of specimen
P_{22} (P_{33})	Compressive strength of specimen
P_{cry}	Crystallization pressure
P_{cry}^{ave}	Average crystallization pressure of all crystals
P_{cry}^{x}	Crystallization pressure generated by phase **x**
$P_{cry,ij}$	Internal stress tensor due to crystallization pressure
P_{ij}	External stress tensor
Q^{ion}	Solubility product
$R_{c/g}$	Volume ratio of the crystal phase to the gel phase
R_g	Gas constant
T	Absolute temperature
V	Total volume of the cement paste sample
v_c	Molar volume of crystal
V_c	Volume of the crystal phase
V_g	Volume of the gel phase
V_p	Volume of the pore space
V_x	Volume of crystal phase **x**
β	Effective stress coefficient of the pore phase
γ	Effective stress coefficient of the crystal phase
$\Delta\phi$	Variation in porosity
ε_{gel}	Strain on the gel phase
ε_{ij}	Strain tensor of the cement paste
κ_{eff}	Volume coefficient of stressed crystal
κ_{shape}	Shape factor of crystal
ν	Poisson's ratio of cement paste
σ_{cry}	Stress on the crystal phase
σ_{gel}	Stress on the gel phase
σ_{ij}''	Biot's effective stress tensor
$\sigma_{ij}''^{0}$	Initial stress tensor
ϕ	Porosity of cement paste

broad dispersion, indicating that it is an amorphous solid with short-range order and long-range disorder [13]. Therefore, the main hydration products of Portland cement can be categorized into two types based on their physical structures: gel products C-S-H [14] and crystal products CH [15]. Research suggests that the strength of cementitious materials results from the precipitation and aggregation of nano-sized C-S-H gel particles [16], while CH contributes to strength by filling voids in the hydration products [17]. Due to the distinct physical and chemical properties of crystals and gels [18], the interactions between these two components in hydration products may affect the mechanical properties of cementitious materials.

The interactions between crystal and gel products, caused by crystallization pressure, induce variations in the internal stress or strain within the hydration products, thereby affecting the properties of cementitious materials [19]. Crystals precipitating from solution can damage the porous materials [20,21], particularly when they grow under external pressure in a supersaturated solution. This phenomenon is known as crystallization pressure [22,23]. In cement paste, gel products form a continuous matrix with pores, while crystal products grow within these pores [17]. During cement hydration, the ions of hydration products remain in a supersaturated state, causing crystals constrained by gel products and generate crystallization pressure [24]. It leads to the interactions between crystal and gel products [19], and further affects the mechanical properties of cementitious materials.

This main purpose of this study is to investigate the impact of crystallization pressure on the interactions between crystal and gel hydration products, and their effect on strength of cementitious materials, through both experimental and theoretical approaches. A mechanism based on crystallization pressure theory was proposed to explain the effect of the interactions between crystal and gel products on the strengths of cementitious materials. Crystallization pressure was varied by immersing specimens in solutions with tailored ion concentration, including water, isopropyl alcohol, ethanol, calcium hydroxide and calcium acetate at different concentrations. Crystallization pressures within the specimens were calculated based on solubility product obtained from inductively-coupled plasma mass spectrometry and ion chromatography tests. Following immersion, the flexural and compressive strengths of these specimens were tested, and the experimental results were analyzed in light of the proposed mechanism. An analytical model was developed to predict the relationship between crystallization pressure and both tensile (flexural) and compressive strengths. This model was validated using experimental results, providing insights into the impact of crystallization pressure on cementitious material strengths.

2. Theoretical principles

Based on the principle of crystallization kinetics, crystallization pressure arises when a crystal grows within a confined space such as a grain boundary or contact area, exerting pressure on the surrounding material [21]. During cement hydration, the ion concentrations of crystal products, such as calcium hydroxide (CH), ettringite (AFt), or monosulfoaluminate (AFm), in the pore solution are typically supersaturated. This supersaturation results in the continuous formation and growth of these crystal products. When the growth of crystal products is restricted by the continuous gel products, such as calcium silicate hydrate (C-S-H) or alumina gel (AH_3), crystallization pressure develops. This crystallization pressure induces the interactions between crystal and gel products, creating a compressive stress state within the crystal products and a tensile stress state within the surrounding gel products [19]. The stress states of hydration products can affect the mechanical properties of cementitious materials. The maximum crystallization pressure P_{cry} of a crystal in solution can be calculated using Eq. 1 [25–27]. Fig. 1 illustrates the simplified model of the interactions in the cementitious materials, along with the resulting mechanical properties and volume changes [19] during hydration process.

$$P_{cry} = \frac{R_g \cdot T}{v_c} \ln\left(\frac{Q^{ion}}{K^{ion}}\right) \tag{1}$$

where, R_g is the gas constant, T is the absolute temperature, v_c is the molar volume of crystal, K^{ion} is the equilibrium solubility, and Q^{ion} is the solubility product.

Based on our previous study [19], it is theoretically inferred that the interactions between crystal and gel products affect the strengths of cement paste throughout the hydration process. The hydration process can be divided into four stages. In **Stage I**, hydration remains limited, and only a small amount of hydration products form. During this stage, the gel products have not yet formed a continuous network, allowing both crystal and gel products to grow freely. As a result, the cementitious materials do not yet harden, and their ability to withstand external loads remains weak. It leads to considerably low compressive and tensile (flexural) strengths of the specimens, with minimal volume changes observed in the specimens.

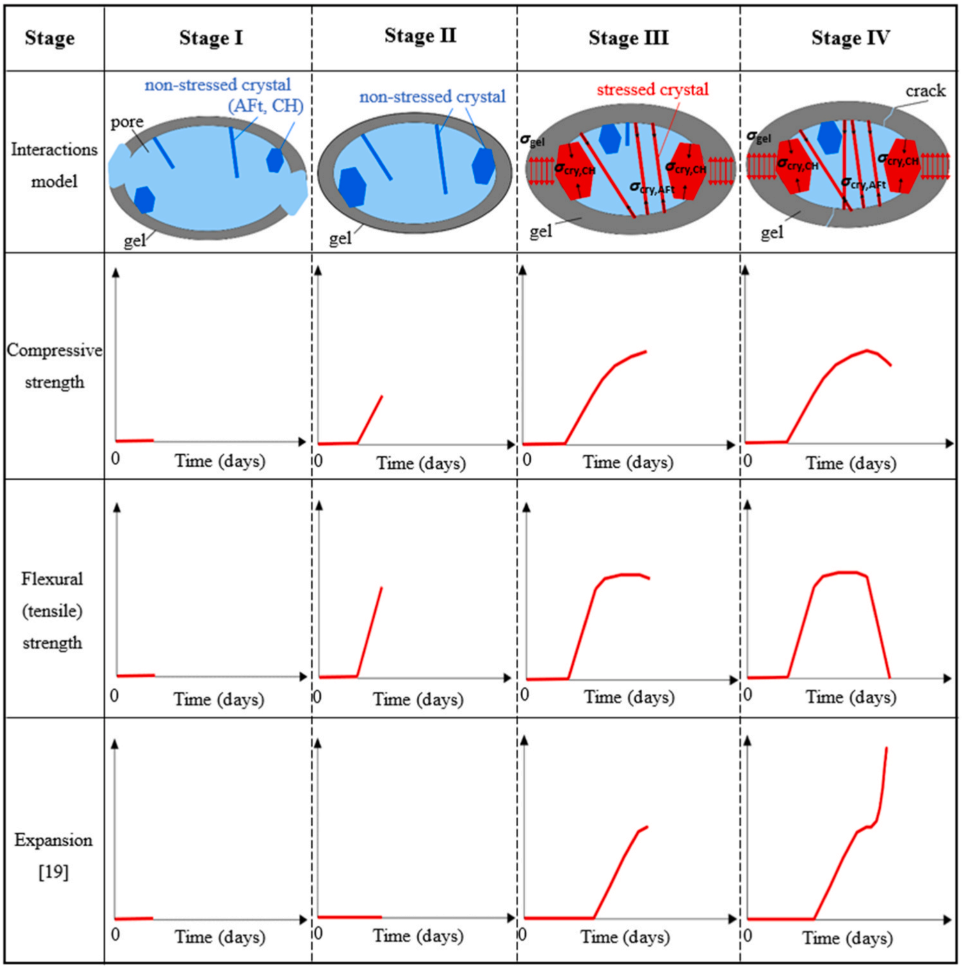

Fig. 1. Simplified model of the interactions in the cementitious materials, the resultant mechanical properties and change in volume[19]. (σ_{cry}=stress of crystal; σ_{gel}=stress of gel).

As hydration progresses beyond **Stage I**, the formation of hydration products accelerates. Consequently, the gel products form a continuous phase, marking the transition to **Stage II**. Although a continuous gel phase is formed, the crystal products are not in contact with the gel products at either end, allowing unrestricted growth. These crystals are defined as non-stressed crystals and are shown in blue color in Fig. 1. As the volume of hydration products increases and porosity decreases, the microstructure becomes denser. This densification enhances resistance to compressive and tensile stresses, thereby improving the mechanical properties of cementitious materials. However, during this stage, the interactions between crystal and gel products do not occur, and only minor volume changes are observed in the specimens.

As hydration continues, the crystal products continued to grow until their growth is restricted by the gel products. This restriction leads to the interactions between crystal and gel products, marking the transition to **Stage III.** During this stage, some non-stressed crystals transform into stressed crystals (red color), applying stress to the surrounding gel products until the maximum crystallization pressure is reached. As hydration progresses, other existing non-stressed crystals or newly generated crystals undergo the similar processes. It further intensifies the interactions between crystal and gel products, creating a greater tensile stress within the surrounding gel products. This tensile stress can potentially reduce the gel's ability to resist external loading, leading to microcrack formation and lowering the tensile strength of the cementitious materials. Additionally, the Poisson effect leads to a decrease in compressive strength. In the early part of **Stage III,** the combined effect of increased hydration products and the interactions between crystal and gel products causes tensile and compressive strengths to continue rising. However, as interactions increase further, the rate of strength gain slows. This effect is more pronounced in tensile strength, which decreases faster than compressive strength, as indicated by the declining flexural-to-compressive strength ratio over time [28,29].

During **Stage III**, the increased interactions between crystal and gel products lead to an increase in the tensile stress within the gel phase, resulting in greater deformation of the gel phase and increased expansion of the overall cementitious materials. Therefore, the cementitious materials expand during **Stage III.**

If the tensile stress within the gel products, resulting from the interactions between crystal and gel products, exceeds its tensile strength, cracking occurs. This marks the transition to **Stage IV**. Due to the increased volume of crystals or the development of crystallization pressure, the interactions between crystal and gel products intensify, leading to crack propagation within the microstructure. It leads to a significant reduction in the tensile and compressive strengths of the cementitious materials. The rate of decrease in flexural strength becomes more pronounced than that of decrease in compressive strength.

During **Stage IV**, the cracked gel phase can no longer restrict the crystal growth. As a result, previously halted crystal growth resumes, leading to the excessive expansion of cementitious materials.

It can be summarized from the above theoretical analysis that increasing the interactions between crystal and gel products leads to greater expansion and a decrease in the tensile (flexural) and compressive strengths of cementitious materials. The impact on tensile (flexural) strength is more pronounced than that on compressive strength.

3. Experimental program

3.1. Experimental design

Based on the analysis in **Section 2**, the interactions between crystal and gel products should be a factor affecting the strength of cementitious materials. Therefore, this study focuses on cementitious materials with a high degree of hydration (the late period of **Stage III**) and regulates crystallization pressure by varying the ion concentration of the pore solution to investigate the influence of the interactions between crystal and gel products on the strength of the cementitious materials. The experimental procedure is illustrated in Fig. 2. First, specimens (cement pastes and mortars) were cast and cured under condition of 98 % relative humidity at 20 ℃ for 1 day. Subsequently, all specimens were submerged in water at 40 ℃ for 28 days curing. After this, the specimens were immersed in different solvents or solutions. Finally, cement mortars were used to test the flexural and compressive strengths, while the cement pastes were used to test the hydration products and pore structure. The ion concentrations in the final solvents or solutions were measured to calculated the crystallization pressure. It is noteworthy that curing in water at 40 ℃ was employed to accelerate the hydration process, minimizing changes in hydrated products and microstructure that might result from continued hydration during the solvent or solution exchange process.

In the experiment, crystallization pressure of crystal products within specimens was altered by varying ion concentrations while immersing specimens in different solvents or solutions. Water and calcium hydroxide solutions were used as control groups to simulate the pore solution conditions of cementitious materials under realistic service environments, providing a baseline for subsequent experiments. Due to the negligible solubility of crystal hydration products in ethanol and isopropyl alcohol, no crystallization pressure is generated in these solvents. As such, they were selected as exchange solvents to eliminate crystallization pressure. To systematically vary the crystallization pressure, calcium acetate solutions with different Ca^{2+} concentrations were prepared. This enabled a quantitative investigation into the impact of crystallization pressure on the mechanical properties of cementitious materials. In addition, all selected solutions and solvents were confirmed to have negligible effects on the hydration products and the microstructure of cement paste. This ensures that the observed changes in mechanical properties can be attributed primarily to crystallization pressure, minimizing interference from other factors [30–34]. Therefore, ethanol and isopropyl alcohol were selected as exchange solvents. Calcium hydroxide, sodium hydroxide, and calcium acetate powders were selected to prepare exchange solutions. Those chemical agents were supplied by local suppliers. The properties of the solvents and solutions are listed in Table 1.

Table 1
Properties of solvents and solutions.

Code	Solvent or solution	Concentration (g/100 g water)	Concentration of Ca^{2+} (mol/L)	Concentration of OH^- (mol/L)
H_2O	water	-	-	-
IPA	isopropyl alcohol	pure	-	-
ETH	ethanol	pure	-	-
CH	calcium hydroxide	0.166 (saturated)	0.0224	0.0448
$CaAc_2$-L	calcium acetate	0.354	0.0224	-
$CaAc_2$-H	calcium acetate	3.54	0.224	-

3.2. Materials and mixture proportions

In this study, Portland cement was utilized with chemical composition detailed in Table 2. The natural river sand with specific gravity of 2.65 g/cm^3 was used as the aggregate.

Cement mortars were prepared for strength testing, while cement pastes were prepared for the examination of hydration products and microstructure. The cement mortars were formulated with a water-to-cement (w/c) ratio of 0.5 and a sand-to-cement (s/c) ratio of 3.0, while the cement pastes were prepared with a w/c ratio of 0.5. A total of eighteen cement mortars and six cement pastes were prepared.

3.3. Sample preparation

The cement mortars were cast in steel molds with dimensions of $40 \times 40 \times 160$ mm^3, while the cement pastes were cast in steel molds with dimensions of $25 \times 25 \times 280$ mm^3. Following casting, the specimens were placed in a curing box maintained at a temperature of 20 ℃ and a relative humidity of 98 %. The specimens were de-moulded after 24 h, and then stored in water at 40 ℃ for 28 days.

3.4. Test methods

3.4.1. Solvent or solution exchange

After curing, all the samples were divided into six groups, each consisting of three mortars and one cement paste. These groups of

Table 2
Primary chemical composition of Portland cement.

Composition	SiO_2	Al_2O_3	Fe_2O_3	CaO	MgO	SO_3
Content (wt%)	20.85	5.28	2.54	61.64	2.58	2.06

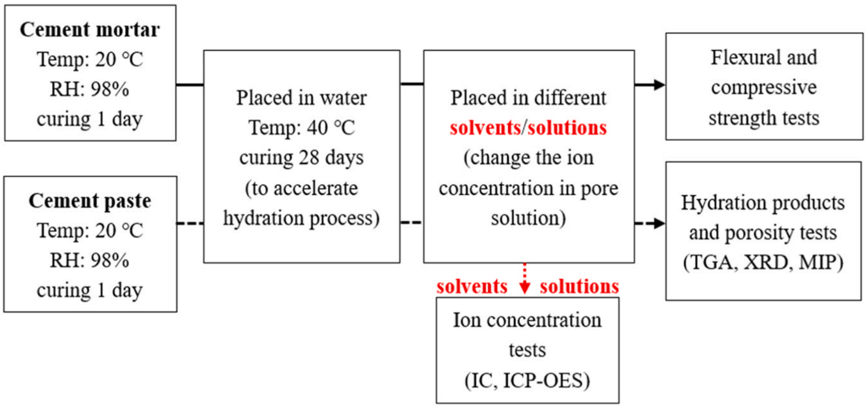

Fig. 2. Flowchart of experimental process. (Temp=temperature; RH=relative humidity; IC=ion chromatography; ICP-OES=inductively-coupled plasma optical emission spectrometry).

specimens were placed in different solvents or solutions (as shown in Table 1) and sealed for pore solution exchange process. The solvents or solutions were renewed every 7 days, and the mass of the specimens was measured until the mass of all specimens remained essentially unchanged.

3.4.2. Mechanical properties test

After solvent or solution exchange process, the flexural and compressive strengths of the mortars were tested. The specimens were split into two parts using three-point bending tests to test the flexural strength. Subsequently, the two split parts were used to test the compressive strength. For each group, three parallel flexural tests and six parallel compressive tests were performed, and the mean values were calculated.

3.4.3. Ion concentration test

The chemical composition of the soaking solution after the pore solution exchange process was analyzed using ion chromatography (IC) and inductively-coupled plasma optical emission spectrometry (ICP-OES). The deionized water used in the laboratory had a conductivity of 18.2 MΩ/cm, and a 0.2 μm disposable microporous filter membrane was used.

3.4.4. Thermogravimetric analysis

Cement pastes from the different groups were subjected to thermogravimetric analysis (TGA). After the solvent or solution exchange process, the cement pastes were crushed and dried in a vacuum drying chamber at 40 ℃. Upon vacuum drying, central fragments of the broken specimens were selected, ground into fine powder using an agate mortar, and then sieved through a 0.056 mm square sieve. The sieved powder was used for the TGA test. The samples obtained after vacuum drying were gradually heated in a controlled N_2 atmosphere at a rate of 10 ℃/min until they reached a temperature of 900 ℃.

3.4.5. X-ray diffraction test

Sample preparation for the X-ray diffraction (XRD) test followed the same method as for TGA. Prior to testing, 10 % α-Al_2O_3 was added as an internal standard. The XRD measurements were conducted within a range of 5°–70°, with a step size of 0.02°.

3.4.6. Mercury intrusion porosimetry test

Mercury intrusion porosimetry (MIP) was performed on the vacuum-dried cement paste samples, which were crushed into pieces measuring 5–7 mm in diameter. The mercury porosimeter was operated within a pressure range of 0.0014–420 MPa. The pore volume was determined by controlling the applied external pressure and the amount of mercury intrusion, and the pore size distribution was represented by either the first-order differential curve or the cumulative distribution curve.

4. Results and discussion

In the study, crystallization pressure was regarded as the primary driving force influencing the interactions between crystal and gel hydration products. Therefore, Ca^{2+} concentration in the pore solution, which directly influenced crystallization pressure, was identified as the critical variable in this experiment. To ensure the stability of the hydration products and minimize the impact of ongoing hydration, specimens with a high degree of hydration were selected. During the solvents/solutions exchange process, the specimens were maintained in a saturated state. In addition, the selected solvents and solutions were specifically chosen to alter the calcium ion concentration without significantly affecting the hydration products or microstructure. Therefore, the variations in mechanical properties could be primarily attributed to differences in crystallization pressure rather than other confounding factors.

4.1. Strengths of specimens after solvents/solutions exchange

The flexural and compressive strengths of the cementitious materials were tested after the pore solution exchange process. To investigate the effect of pore solution composition on the mechanical properties of the cementitious materials, the flexural and compressive strengths of specimens immersed in water were considered as the reference strengths (set to 1). The standardized strengths of specimens immersed in other solutions (e.g., calcium hydroxide and calcium acetate) or solvents (e.g., ethanol and isopropyl alcohol) were compared with the reference strength, with the results presented in Table 3. As shown in Table 3, both the flexural and compressive strengths of the specimens with ethanol and isopropyl alcohol as pore solutions were higher than the reference strengths (those of the water-immersed specimens). The flexural and compressive strengths of the specimens immersed in calcium hydroxide and low-concentration calcium acetate solutions were similar to the reference strengths. Specimens immersed in high-concentration calcium acetate solutions exhibited lower flexural and compressive strengths compared to the reference strengths, with a more significant decrease in flexural strength. In various solutions (or solvents), differences in ion concentrations of crystal products affect crystallization pressure, leading to variations in the interactions between crystal and gel products. This may explain the differences in the strength of cementitious materials after immersion in different solutions or solvents. The crystallization pressure of crystal products in cement mortar immersed in different solvents or solutions was determined by ion concentration test.

4.2. Hydration products, porosity and crystallization pressure for different specimens

The TGA curves, XRD patterns and pore size distributions of specimens were obtained, which demonstrated that the hydration products and porosity of cement pastes immersed in various solvents or solutions remained largely unaffected [19]. This finding is consistent with results reported in the literature [30–34]. It indicates the observed differences in the strengths of the cementitious materials after solvent or solution exchange are primarily attributed to changes in the interactions between crystal and gel hydration products. The types and contents of hydration products in the specimens immersed in different solvents or solutions are listed in Table 4 [19].

For Portland cement, the primary crystal hydration products are calcium hydroxide, ettringite and AFm, which consist of Ca^{2+}, OH^-, AlO_2^- and SO_4^{2-} ions. The ion concentrations in different exchange solvents or solutions also have been reported in our previous study [19]. Since the hydration products AFt, AFm, and CH generate crystallization pressure in Portland cementitious materials, the average crystallization pressure was used to characterize the pressure within the specimens. It was defined as follows [19]:

$$P_{\text{cry}}^{\text{ave}} = \frac{\kappa_{\text{shape,CH}} \cdot P_{\text{cry}}^{\text{CH}} V_{\text{CH}} + \kappa_{\text{shape,AFt}} \cdot P_{\text{cry}}^{\text{AFt}} V_{\text{AFt}} + \kappa_{\text{shape,AFm}} P_{\text{cry}}^{\text{AFm}} V_{\text{AFm}}}{V_{\text{CH}} + V_{\text{AFt}} + V_{\text{AFm}}} \tag{2}$$

Table 3
Comparison of standardized flexural and compressive strengths with the reference strengths.

Specimen	Solvents or solutions	Standardized flexural strength (-)	Standardized compressive strength (-)
H_2O	water	1 (reference strength)	1 (reference strength)
IPA	isopropyl alcohol	1.24	1.08
ETH	ethanol	1.29	1.11
CH	calcium hydroxide	1.08	1.01
$CaAc_2$-L	calcium acetate	1.01	0.96
$CaAc_2$-H	calcium acetate	0.86	0.95

Table 4
Types and contents of hydration products in specimens immersed in different solvents or solutions [15].

Phase	C-S-H	CH	AFt	AFm
Content (wt%)	44.76	22.15	6.59	3.98

where, $P_{\mathrm{cry}}^{\mathrm{ave}}$ denotes the average crystallization pressure of all crystals; V_{x} denotes the volume of crystal phase x; $P_{\mathrm{cry}}^{\mathrm{x}}$ denotes the crystallization pressure generated by phase x; κ_{shape} is the shape factor, and its values for AFt, CH and AFm are set to 1, 2/3 and 2/3, respectively.

The Average crystallization pressure for different specimens were calculated and are provided in Table 5.

4.3. *Effects of crystallization pressure on the strengths of cementitious materials*

Table 3 and Table 5 reveal that the specimens with crystallization pressures of 101.7 MPa and 147.8 MPa exhibited reductions in tensile (flexural) strength by 19.34 % and 30.65 %, respectively, and decreases in compressive strength by 10.00 % and 14.41 %, respectively, compared to the specimens with zero crystallization pressure. These findings indicate that both the calculated and experimentally measured tensile and compressive strengths of the specimens increased as crystallization pressure decreased. This trend suggests that the stronger interactions between crystal and gel products lead to a reduction in the strengths of cementitious materials. Notably, the reduction in tensile strength was more significant than that in compressive strength.

In cementitious materials, the interactions between crystal and gel products influence the internal stress states of the hydration products, resulting in tensile stress in gel products and compressive stress in the crystal products. Consequently, the interactions between crystal and gel phases in cementitious materials induce internal stress within the hydration products, even in the absence of external force. This internal stress can be considered analogous to “prestress”. When external forces are applied, the hydration products experience a superposition of stresses arising from both the external load and the internal interactions between crystal and gel phases. Given the inherent brittleness of cementitious materials, they are particularly susceptible to failure under tensile stress. The tensile “prestress” in gel products, resulting from the interactions between crystal and gel products, diminishes the capacity of the gel products to withstand external tensile stress. When the stress in gel products exceeds its own tensile strength, cracking occurs within the gel phases. The heightened cracking and increased susceptibility to damage in the gel products can lead to the formation of microcracks within the cementitious materials, ultimately compromising the structural integrity and increasing the risk of macrocrack development. Consequently, an increase in the interactions between crystal and gel products correlates with a reduction in the strengths of cementitious materials.

5. Analytical model

5.1. *Model development*

Based on the principles of poroelasticity [35], a relationship was established between the strengths of the cement paste and the interactions between crystal and gel products. It is detailed as follows.

Table 5
Average crystallization pressure for different specimens.

Code	H_2O	IPA	ETH	CH	$CaAc_2$-L	$CaAc_2$-H
Average crystallization pressure (MPa)	101.7	0	0	104.0	109.3	147.8

Note: H_2O=water; IPA=isopropyl alcohol; ETH=ethanol; CH=calcium hydroxide; $CaAc_2$=calcium acetate; L=low concentration; H=high concentration.

Consider a cement paste sample with volume V, comprising a gel phase (V_{g}), a crystal phase (V_{c}), and an interconnected pore space (V_{p}). The total volume is the sum of the three volumes:

$$V = V_{\mathrm{g}} + V_{\mathrm{c}} + V_{\mathrm{p}} \tag{3}$$

The porosity ϕ is defined as:

$$\phi = \frac{V_{\mathrm{p}}}{V} = \frac{V_{\mathrm{p}}}{V_{\mathrm{g}} + V_{\mathrm{c}} + V_{\mathrm{p}}} \tag{4}$$

Under uniaxial stress, the combined effect of external forces and the interactions between crystal and gel products within the cement paste leads to deformation. Neglecting the effects of the temperature changes and hydrostatic pressure, the strain tensor of the cement paste ($\varepsilon_{\mathrm{ij}}$) can be expressed as [36]:

$$\varepsilon_{11} = \frac{1}{E}\left(\sigma_{11}{}'' - \sigma_{11}{}''^{0}\right) - \frac{\nu}{E}\left(\sigma_{22}{}'' - \sigma_{22}{}''^{0}\right) - \frac{\nu}{E}\left(\sigma_{33}{}'' - \sigma_{33}{}''^{0}\right) \tag{5}$$

$$\varepsilon_{22} = \frac{1}{E}\left(\sigma_{22}{}'' - \sigma_{22}{}''^{0}\right) - \frac{\nu}{E}\left(\sigma_{11}{}'' - \sigma_{11}{}''^{0}\right) - \frac{\nu}{E}\left(\sigma_{33}{}'' - \sigma_{33}{}''^{0}\right) \tag{6}$$

$$\varepsilon_{33} = \frac{1}{E}\left(\sigma_{33}{}'' - \sigma_{33}{}''^{0}\right) - \frac{\nu}{E}\left(\sigma_{11}{}'' - \sigma_{11}{}''^{0}\right) - \frac{\nu}{E}\left(\sigma_{22}{}'' - \sigma_{22}{}''^{0}\right) \tag{7}$$

where, $\varepsilon_{\mathrm{ij}}$ denotes the strain tensor of cement paste, $\sigma_{\mathrm{ij}}^{''}$ denotes Biot’s effective stress tensor, $\sigma_{\mathrm{ij}}^{''0}$ denotes initial stress tensor, E is the elastic modulus of cement paste, and ν is the Poisson’s ratio.

Under uniaxial stress, the external stress (P) is normal stress acting along a single axis of the material. Therefore,

$$P_{\mathrm{ij}} = P \quad (\mathrm{i} = \mathrm{j} = 1); \quad P_{\mathrm{ij}} = 0 \quad (\mathrm{i},\ \mathrm{j} \neq 1) \tag{8}$$

The internal stress is driven by the crystallization pressure. It was assumed that the crystallization pressure acted uniformly on the pore walls. Therefore, the internal stress tensor ($P_{\mathrm{cry,ij}}$) can be expressed as:

$$P_{\mathrm{cry,ij}} = \kappa_{\mathrm{eff}} P_{\mathrm{cry}} \quad (\mathrm{i} = \mathrm{j}); \quad P_{\mathrm{cry,ij}} = 0 \quad (\mathrm{i} \neq \mathrm{j}) \tag{9}$$

where, κ_{eff} is the volume coefficient of stressed crystals and P_{cry} is the crystallization pressure.

Based on poroelasticity, the strains of the cement paste, pores, and crystals were:

The strain on cement paste:

$$\varepsilon_{11} = \frac{1}{E}\left(P + \alpha\kappa_{\mathrm{eff}} P_{\mathrm{cry}} - 2\nu\alpha\kappa_{\mathrm{eff}} P_{\mathrm{cry}}\right) \tag{10}$$

$$\varepsilon_{22} = \varepsilon_{33} = \frac{1}{E}\left(\alpha\kappa_{\mathrm{eff}} P_{\mathrm{cry}} - \nu P - 2\nu\alpha\kappa_{\mathrm{eff}} P_{\mathrm{cry}}\right) \tag{11}$$

The strain on pores:

$$\varepsilon_{11}^{\mathrm{pore}} = \frac{1}{E_{\mathrm{p}}}\left(P + \beta\kappa_{\mathrm{eff}} P_{\mathrm{cry}} - 2\nu\beta\kappa_{\mathrm{eff}} P_{\mathrm{cry}}\right) \tag{12}$$

$$\varepsilon_{22}^{\mathrm{pore}} = \varepsilon_{33}^{\mathrm{pore}} = \frac{1}{E_{\mathrm{p}}}\left(\beta\kappa_{\mathrm{eff}} P_{\mathrm{cry}} - \nu P - 2\nu\beta\kappa_{\mathrm{eff}} P_{\mathrm{cry}}\right) \tag{13}$$

The strain on crystals:

$$\varepsilon_{11}^{\mathrm{crystal}} = \frac{1}{E_{\mathrm{cry}}}\left(P + \gamma\kappa_{\mathrm{eff}} P_{\mathrm{cry}} - 2\nu\gamma\kappa_{\mathrm{eff}} P_{\mathrm{cry}}\right) \tag{14}$$

$$\varepsilon_{22}^{\mathrm{crystal}} = \varepsilon_{33}^{\mathrm{crystal}} = \frac{1}{E_{\mathrm{cry}}}\left(\gamma\kappa_{\mathrm{eff}} P_{\mathrm{cry}} - \nu P - 2\nu\gamma\kappa_{\mathrm{eff}} P_{\mathrm{cry}}\right) \tag{15}$$

where, β and γ are the effective stress coefficients of the pore and crystal phases, respectively, and E_{p} and E_{cry} denote the elastic moduli of the pore and crystal phases, respectively.

The variation in porosity $\Delta\phi$ can be obtained as follows:

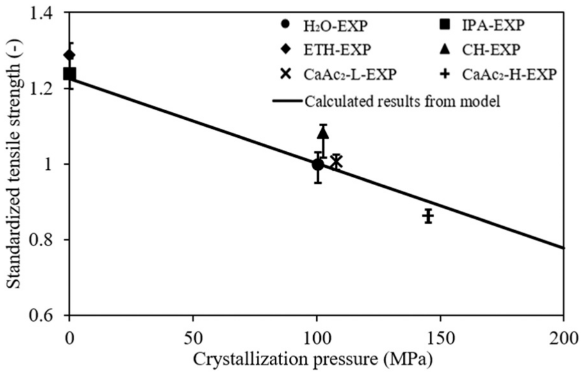

Fig. 3. Comparison between experimental and calculated standardized tensile strengths of samples subjected to different crystallization pressures. (EXP= experimental results; H_2O=water; IPA=isopropyl alcohol; ETH=ethanol; CH=calcium hydroxide; $CaAc_2$=calcium acetate; L=low concentration; H=high concentration).

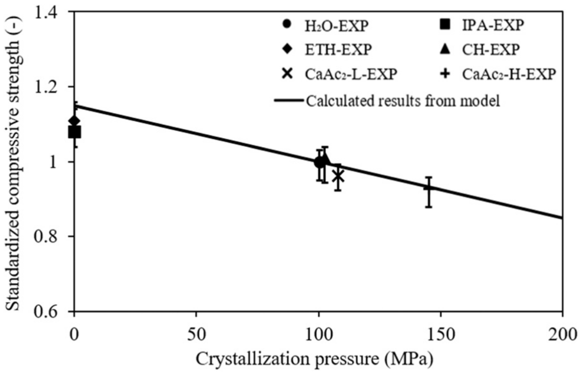

Fig. 4. Comparison between experimental and calculated standardized compressive strengths of samples subjected to different crystallization pressures. (EXP= experimental results; H_2O=water; IPA=isopropyl alcohol; ETH=ethanol; CH=calcium hydroxide; $CaAc_2$=calcium acetate; L=low concentration; H=high concentration).

$$\Delta\phi = \Delta\left(\frac{V_p}{V}\right) = \frac{\Delta V_p - \phi\Delta V}{V} \tag{16}$$

The following set of kinematic relations can be derived based on Eq. (3):

$$\varepsilon = \frac{\Delta V}{V} = \frac{\Delta V_g + \Delta V_c}{V_g + V_c} + \frac{\Delta\phi}{1-\phi} \tag{17}$$

$$\varepsilon^{pore} = \frac{\Delta V_p}{V_p} = \frac{\Delta V_g + \Delta V_c}{V_g + V_c} + \frac{\Delta\phi}{(1-\phi)\phi} \tag{18}$$

The relationship between stress and strain on gel products is:

$$\varepsilon^{gel} = \frac{\Delta V_g}{V_g} = \frac{\sigma_{gel}}{E_{gel}} \tag{19}$$

where, ε_{gel} and σ_{gel} denote the strain and stress on the gel phase, respectively, and E_{gel} denotes its elastic modulus.

Therefore, considering the role of the interactions between crystal and gel products, the relationships between the strain and internal and external stresses on the cement paste are as follows:

$$P_{11} = \left\{\frac{\sigma_{gel}(1-\phi)}{E_{gel}\left(1+R_{c/g}\right)} - (1-2\nu)\kappa_{eff}P_{cry}\left[\frac{\alpha}{E} - \frac{\beta\phi}{E_p} - \frac{\gamma R_{c/g}(1-\phi)}{\left(1+R_{c/g}\right)E_c}\right]\right\}\cdot K^{-1} \tag{20}$$

where, ϕ is the porosity of cement paste.

In this study, it is considered that the matrix fails when the stress generated by the gel products reaches its own tensile strength. At this point, the external stresses P_{11} and P_{22} (P_{33}) correspond to the tensile and compressive strengths of specimen, respectively.

5.2. Model verification

The model was validated using experimental data from **Section 4**. Based on Eqs. (20) and (21), the tensile and compressive strengths (also expressed in terms of reference strengths) with different crystallization pressures were calculated and compared with the experimental results, as shown in Fig. 3 and Fig. 4, respectively. The tensile strength of C-S-H is 66–320 MPa [37], and the elastic modulus of C-S-H, CH, AFt and AFm are 20–30 GPa [37], 35–51 GPa [38], 22.4 GPa [39] and 42.3 GPa [39], respectively. The Poisson's ratio of cement paste ranges from 0.25 to 0.3 [40]. Variations in the tensile strength of cementitious materials were assessed through changes in flexural strength.

The results presented in Fig. 3 and Fig. 4 indicate that the calculated values generally aligned with the experimental trends, confirming a linear relationship between crystallization pressure and strengths. Both tensile (flexural) and compressive strengths decreased with increasing crystallization pressure. The results confirm the accuracy of the model. Drawing from both experimental findings and the analytical model, ion concentrations in the pore solution influence the crystallization pressure of crystal products in cementitious materials, thereby affecting their strengths. Higher crystallization pressure led to stronger interactions between crystal and gel products, ultimately resulting in a reduction in both tensile and compressive strengths.

$$P_{22} = P_{33} = \left\{(1-2\nu)k_{eff}P_{cry}\left[\frac{\alpha}{E} - \frac{\beta\phi}{E_p} - \frac{\gamma R_{c/g}(1-\phi)}{\left(1+R_{c/g}\right)E_c}\right] - \frac{\sigma_{gel}(1-\phi)}{E_{gel}\left(1+R_{c/g}\right)}\right\}\cdot(\nu K)^{-1} = -\frac{P_{11}}{\nu} \tag{21}$$

where, $R_{c/g}$ is the volume ratio of the crystal to the gel phase, K is a parameter related to the elastic modulus, $R_{c/g}$, and porosity, and it is defined as follows:

$$K = \frac{1}{E} - \frac{\phi}{E_p} - \frac{R_{c/g}(1-\phi)}{\left(1+R_{c/g}\right)E_c} \tag{22}$$

Moreover, κ_{eff} denotes the volume coefficient of stressed crystals and. According to our previous study [19], it can be expressed as:

$$K_{eff} = 1 - e^{-\frac{0.3}{\phi}} \tag{23}$$

5.3. Moisture-induced weakening based on the interactions between crystal and gel hydration products

Cementitious materials often remain in a wet or even saturated state due to the diffusion of moisture from the air into the concrete interior or through water penetration in hydraulic structures. A negative correlation has been established between the internal moisture content of cementitious materials and their mechanical properties [41–43]. This phenomenon is known as moisture-induced weakening (or water-rock interactions). The mechanism of moisture-induced weakening is approximately summarized into two categories: the corrosive action of water and the mechanical action of water [44–47]. Concrete sleepers have been reported to corrode due to the flow of abrasive liquids, contributing to concrete deterioration [48]. However, experiments controlling the internal water content of concrete through relative humidity indicate that in the absence of flowing water, the strength of concrete decreases as pore water saturation increases [41]. It suggests that matrix corrosion due to flowing water is not the sole factor in the strength reduction of cementitious materials. Some studies suggest that moisture-induced weakening occurs because surface shrinkage induces biaxial compression in the specimen’s core, which increases its strength in the third direction, that is, in the direction of the applied load. In addition, Capillary forces, a type of mechanical effect, arise during the evaporation of free water in capillary pores. These forces induce shrinkage stress, compacting the matrix and thereby increasing strength [45]. However, experimental results showed that well-cured concrete, when completely dry and free from significant shrinkage (in the absence of biaxial stress), exhibits higher compressive strength than when tested in a wet condition [49]. Therefore, the mechanical action of water on the mechanical properties of cementitious materials remains less explored [41].

In this study, an increase in the interactions between crystal and gel products, driven by crystallization pressure, is shown to reduce the strength of cementitious materials. It has been established that crystallization pressure arises when a thin fluid layer exists at the crystal-solid interface, facilitating mass transport for crystal growth [21,25]. In dry cementitious materials, the thin fluid layer disappears, and the crystallization pressure is absent. As a result, there are no interactions between crystal and gel products [19]. Consequently, the strength of dry cementitious materials surpasses that of water-saturated cementitious materials. Research indicates that the compressive strength of cementitious materials in dry conditions is 10–20 % higher than that in saturated conditions [50–54]. These findings align with the experimental and calculated results in this study, which compare fully saturated specimens (immersed in water) to those without interactions between crystal and gel products (immersed in isopropyl alcohol or ethanol). Therefore, variations in the interactions between crystal and gel products represent a critical factor influencing the mechanical properties of cementitious materials with different moisture contents.

6. Conclusions

This study investigates the impact of crystallization pressure on the interactions between crystal and gel hydration products and the mechanical properties of cementitious materials through solution exchange experiments and theoretical analysis. The following conclusions are drawn.

(1) Ion concentrations in the pore solution of cementitious materials is altered by immersing them in different solvents or solutions (such as water, isopropyl alcohol, ethanol, calcium hydroxide and calcium acetate with various concentrations), which in turn changes the crystallization pressure of crystal products and ultimately affects both the flexural and compressive strengths.

(2) The interactions between crystal and gel products affects the mechanical properties of cementitious materials. Crystallization pressure, which directly affects the interactions, negatively impacts the strengths of cementitious materials. Compared to the reference specimens with zero crystallization pressure, specimens with crystallization pressures of 101.7 and 147.8 MPa exhibited reductions in flexural strength by 19.34 % and 30.65 %, respectively, and decreases in compressive strength by 10.00 % and 14.41 %. These findings indicate that both tensile and compressive strengths improve as crystallization pressure decreases, with the reduction in flexural strength being more pronounced than that in compressive strength. Theoretical analysis indicates that the interactions induce tensile stress within the gel products even in the absence of external loading. This resembles a tensile "prestress" that diminishes the gel products’ capacity to withstand external tensile loads, thereby reducing their strengths.

(3) The analytical model developed in this study examines the mechanical properties of cementitious materials based on the interactions between crystal and gel products. The model indicates that the strengths of cementitious materials are influenced by factors such as the volume ratio of the crystal to the gel phase, porosity and crystallization pressure. The tensile and compressive strengths predicted by the model align well with the experimental results, thus validating the model’s accuracy.

The interactions between crystal and gel products driven by crystallization pressure affects the mechanical properties. It can explain the “moisture-induced weakening” phenomenon observed in engineering. This finding provides a new perspective for understanding the influence of moisture content on the mechanical properties of inorganic porous materials.

Future work

The Poisson’s ratio of cementitious materials changes during the hydration process. Similarly, the interactions between crystal and gel products may also influence the Poisson’s ratio. However, the effect of the interactions between crystal and gel products on the Poisson’s ratio was not considered in this study. Therefore, in future work, we will analyze the effect of the interactions between crystal gel and the product on the Poisson’s ratio of cementitious materials to further refine the established model.

In addition, the mechanism and model proposed in this study provide a theoretical basis for understanding the durability of porous materials, particularly with respect to salt erosion damage, which will be addressed in future studies.

CRediT authorship contribution statement

Zhang Depeng: Writing – original draft, Validation, Methodology, Conceptualization. **Pi Zhenyu:** Writing – review & editing, Methodology. **Li Hui:** Writing – review & editing, Methodology. **Xu Mingfeng:** Writing – review & editing, Funding acquisition. **Zhou Jian:** Supervision, Resources, Funding acquisition, Conceptualization. **Ye Guang:** Writing – review & editing. **Zhang Mingzhong:** Writing – review & editing.

Declaration of Competing Interest

The authors declare that they have no known competing financial interests or personal relationships that could have appeared to influence the work reported in this paper.

Acknowledgments

This research was supported by the National Natural Science Foundation of China (Grant Nos. 52293434 and 52178200), the Natural Science Foundation of Hebei Province, China (No. E2022202124), and the China Scholarship Council.

Data availability

Data will be made available on request.

References

[1] R.F. Feldman, J.J. Beaudoin, Microstructure and strength of hydrated cement, Cem. Concr. Res. 6 (1976) 389–400, https://doi.org/10.1016/0008-8846(76)90102-2.

[2] P. Wang, F. Bernard, S. Kamali-Bernard, Mechanical properties of calcium-silicate-hydrates (CSH) gel colloid at sub-micro scale by using molecular dynamics based cohesive zone representation of inter-globule interaction, Constr. Build. Mater. 416 (2024) 134683, https://doi.org/10.1016/j.conbuildmat.2023.134683.

[3] M. Zhang, L. Yang, F. Wang, Understanding the longer-term effects of C–S–H seeding materials on the performance of limestone calcined clay cement, Constr. Build. Mater. 392 (2023) 131829, https://doi.org/10.1016/j.conbuildmat.2023.131829.

[4] J. Wang, S. Ding, F. Du, et al., Interaction between calcium hydroxide and calcium-alumino-silicate-hydrate on micromechanical properties, Constr. Build. Mater. 449 (2024) 138321, https://doi.org/10.1016/j.conbuildmat.2024.138321.

[5] T. Dorn, O. Blask, D. Stephan, Acceleration of cement hydration–A review of the working mechanisms, effects on setting time, and compressive strength development of accelerating admixtures, Constr. Build. Mater. 323 (2022) 126554, https://doi.org/10.1016/j.conbuildmat.2022.126554.

[6] Q. Luo, Y. Xiang, Q. Yang, et al., Molecular simulation of calcium-silicate-hydrate and its applications: a comprehensive review, Constr. Build. Mater. 409 (2023) 134137, https://doi.org/10.1016/j.conbuildmat.2023.134137.

[7] H.M. Jennings, Refinements to colloid model of CSH in cement: CM-II, Cem. Concr. Res. 38 (2008) 275–289, https://doi.org/10.1016/j.cemconres.2007.10.006.

[8] P. Gao, G. Ye, J. Wei, et al., Extension of the Hymostruc3D model for simulation of hydration and microstructure development of blended cements, Heron 64 (2019) 125–148. ⟨http://resolver.tudelft.nl/uuid:7355227e-021b-4356-8a9c-ccacf2e44b28⟩.

[9] I. Odler, Strength of cement, Mater. Struct. 24 (1991) 143–157, https://doi.org/10.1007/BF02472476.

[10] T.C. Powers, T.L. Brownyard, Studies of the physical properties of hardened Portland cement paste, J. Am. Concr. Inst. 43 (1947) 549–602.

[11] P. Termkhajornkit, Q.H. Vu, R. Barbarulo, et al., Dependence of compressive strength on phase assemblage in cement pastes: beyond gel–space ratio—Experimental evidence and micromechanical modeling, Cem. Concr. Res. 56 (2014) 1–11, https://doi.org/10.1016/j.cemconres.2013.10.007.

[12] B. Pichler, C. Hellmich, J. Eberhardsteiner, et al., Effect of gel–space ratio and microstructure on strength of hydrating cementitious materials: an engineering micromechanics approach, Cem. Concr. Res. 45 (2013) 55–68, https://doi.org/10.1016/j.cemconres.2012.10.019.

[13] K. Mather, Examination of Cement Pastes, Hydrated Pastes, and Synthetic Products by X-ray Diffraction, Evaluation of Methods of Identifying Phases of Cement Paste, Transportation Research Circular No. 176, Transportation Research Board, Washington, DC, pp. 9 – 30.

[14] I.G. Richardson, The nature of the hydration products in hardened cement pastes, Cem. Concr. Compos. 22 (2000) 97–113, https://doi.org/10.1016/S0958-9465(99)00036-0.

[15] Y. Zhang, X. Kong, L. Chen, et al., Influence of triethanolamine on the hydration product of portlandite in cement paste and the mechanism, Cem. Concr. Res. 87 (2016) 64–76, https://doi.org/10.1016/j.cemconres.2016.05.009.

[16] E. Masoero, E. Del Gado, R.J.M. Pellenq, Nanostructure and nanomechanics of cement: polydisperse colloidal packing, Phys. Rev. Lett. 109 (2012) 155503, https://doi.org/10.1103/PhysRevLett.109.155503.

[17] C. Carde, R. François, Effect of the leaching of calcium hydroxide from cement paste on mechanical and physical properties, Cem. Concr. Res. 27 (1997) 539–550, https://doi.org/10.1016/S0008-8846(97)00042-2.

[18] M. Steiger, Crystal growth in porous materials—I: the crystallization pressure of large crystals, J. Cryst. Growth 282 (2005) 455–469, https://doi.org/10.1016/j.jcrysgro.2005.05.007.

[19] D. Zhang, H. Li, Z. Pi, et al., Effect of the interactions between crystal and gel hydration products on the volume change of cementitious materials, Cem. Concr. Compos 154 (2024) 105764, https://doi.org/10.1016/j.cemconcomp.2024.105764.

[20] A. Stahlbuhk, M. Steiger, Damage potential and supersaturation of nitrates relevant to salt damage of porous building materials, Constr. Build. Mater. 419 (2024) 135413, https://doi.org/10.1016/j.conbuildmat.2024.135413.

[21] L. Li, F. Kohler, J. Dziadkowiec, et al., Limits to crystallization pressure, Langmuir 38 (2022) 11265–11273, https://doi.org/10.1021/acs.langmuir.2c01325.

[22] S. Taber, The growth of crystals under external pressure, Am. J. Sci. (246) (1916) 532–556, https://doi.org/10.2475/ajs.s4-41.246.532.

[23] Q. Xiong, L. Tong, J. Huang, et al., Salt crystallization in porous materials: a quasi-local transport model for evaluating pore filling process, Constr. Build. Mater. 462 (2025) 139904, https://doi.org/10.1016/j.conbuildmat.2025.139904.

[24] G.W. Scherer, Stress from crystallization of salt, Cem. Concr. Res. 34 (2004) 1613–1624, https://doi.org/10.1016/j.cemconres.2003.12.034.

[25] C.W. Correns, Growth and dissolution of crystals under linear pressure, Discuss. Faraday Soc. 5 (1949) 267–271, https://doi.org/10.1039/DF9490500267.

[26] J.W. Cahn, Surface stress and the chemical equilibrium of small crystals—I. The case of the isotropic surface, Acta Met. 28 (1980) 1333–1338, https://doi.org/10.1016/0001-6160(80)90002-4.

[27] J.F. Georgin, N. Maach, J. Pommay, Sulphate crystallization modelling and surface reactivity in solution, Constr. Build. Mater. 156 (2017) 266–276, https://doi.org/10.1016/j.conbuildmat.2017.08.155.

[28] D. Teo, C. Lee, T.S. Lee, The effect of aggregate condition during mixing on the mechanical properties of oil palm shell (OPS) concrete, Matec. Web. Conf. 87 (2017) 1–4, https://doi.org/10.1051/matecconf/20178701019.

[29] Y. Wang, J. Li, L. Jiang, et al., Enhanced mechanical and microstructural properties of Portland cement composites modified with submicron metakaolin, Adv. Civ. Eng. 2020 (2020) 1–13, https://doi.org/10.1155/2020/8882385.

[30] X. Wang, A.B. Eberhardt, E. Gallucci, et al., Assessment of early age properties of cementitious system through isopropanol–water replacement in the mixing water, Cem. Concr. Res. 84 (2016) 76–84, https://doi.org/10.1016/j.cemconres.2016.02.009.

[31] J. Zhang, G.W. Scherer, Comparison of methods for arresting hydration of cement, Cem. Concr. Res. 41 (2011) 1024–1036, https://doi.org/10.1016/j.cemconres.2011.06.003.

[32] Z. Zhang, G.W. Scherer, Supercritical drying of cementitious materials, Cem. Concr. Res. 99 (2017) 137–154, https://doi.org/10.1016/j.cemconres.2017.05.005.

[33] K. Cao, L. Wang, Y. Xu, et al., The hydration and compressive strength of cement mortar prepared by calcium acetate solution, Adv. Civ. Eng. 2021 (2021) 1–9, https://doi.org/10.1155/2021/8817725.

[34] N.C. Collier, J.H. Sharp, N.B. Milestone, et al., The influence of water removal techniques on the composition and microstructure of hardened cement pastes, Cem. Concr. Res. 38 (2008) 737–744, https://doi.org/10.1016/j.cemconres.2008.02.012.

[35] Y. Gu, P. Dangla, R.-P. Martin, et al., Modeling the sulfate attack induced expansion of cementitious materials based on interface-controlled crystal growth mechanisms, Cem. Concr. Res. 152 (2022) 106676, https://doi.org/10.1016/j.cemconres.2021.106676.

[36] O. Coussy, Poromechanics, John Wiley & Sons Ltd., Chichester, 2004, https://doi.org/10.1002/0470092718.fmatter.

[37] M. Hlobil, V. Šmilauer, G. Chanvillard, Micromechanical multiscale fracture model for compressive strength of blended cement pastes, Cem. Concr. Res. 83 (2016) 188–202, https://doi.org/10.1016/j.cemconres.2015.12.003.

[38] J.J. Chen, L. Sorelli, M. Vandamme, et al., A coupled nanoindentation/SEM-EDS study on low water/cement ratio Portland cement paste: evidence for CSH/Ca(OH)2 nanocomposites, J. Am. Ceram. Soc. 93 (2010) 1484–1493, https://doi.org/10.1111/j.1551-2916.2009.03599.x.

[39] S. Kamali, M. Moranville, E. Garboczi, et al., Hydrate dissolution influence on the Young's modulus of cement pastes, Proceedings of the 5th International Conference on Fracture Mechanics of Concrete and Concrete Structures, Vail, USA, 2004, pp. 631–638.

[40] C.-J. Haecker, E.J. Garboczi, J.W. Bullard, et al., Modeling the linear elastic properties of Portland cement paste, Cem. Concr. Res. 35 (2005) 1948–1960, https://doi.org/10.1016/j.cemconres.2005.05.001.

[41] W. Wang, C. Lu, G. Yuan, et al., Effects of pore water saturation on the mechanical properties of fly ash concrete, Constr. Build. Mater. 130 (2017) 54–63, https://doi.org/10.1016/j.conbuildmat.2016.11.031.

[42] P.G. Ranjith, D. Jasinge, J.Y. Song, et al., A study of the effect of displacement rate and moisture content on the mechanical properties of concrete: use of acoustic emission, Mech. Mater. 40 (2008) 453–469, https://doi.org/10.1016/j.mechmat.2007.11.002.

[43] H. Haddad, M. Al Kobaisi, Influence of moisture content on the thermal and mechanical properties and curing behavior of polymeric matrix and polymer concrete composite, Mater. Des. 49 (2013) 850–856, https://doi.org/10.1016/j.matdes.2013.01.075.

[44] W. Ren, J. Xu, J. Liu, et al., Dynamic mechanical properties of geopolymer concrete after water immersion, Ceram. Int. 41 (2015) 11852–11860, https://doi.org/10.1016/j.ceramint.2015.05.154.

[45] S. Wu, X. Chen, J. Zhou, Influence of strain rate and water content on mechanical behavior of dam concrete, Constr. Build. Mater. 36 (2012) 448–457, https://doi.org/10.1016/j.conbuildmat.2012.06.046.

[46] I.M. Nikbin, M.H.A. Beygi, M.T. Kazemi, et al., A comprehensive investigation into the effect of water to cement ratio and powder content on mechanical properties of self-compacting concrete, Constr. Build. Mater. 57 (2014) 69–80, https://doi.org/10.1016/j.conbuildmat.2014.01.098.

[47] M. Nematzadeh, M. Naghipour, Compressing fresh concrete technique and the effect of excess water content on physical–mechanical properties of compressed concrete, Mater. Des. 37 (2012) 256–267, https://doi.org/10.1016/j.matdes.2011.12.051.

[48] J. César Bastos, M.S. Dersch, J.R. Edwards, Degradation mechanisms of concrete due to water flow in cracks of prestressed railroad sleepers under cyclic loading, J. Mater. Civ. Eng. 34 (2022) 04022025, https://doi.org/10.1061/(ASCE)MT.1943-5533.0004144.

[49] F.M. Bartlett, J.G. MacGregor, Effect of moisture condition on concrete core strengths, Acids Mater. J. 91 (1994) 227–236.

[50] F. Wittmann, Surface tension skrinkage and strength of hardened cement paste, Mater. Struct. 1 (1968) 547–552, https://doi.org/10.1007/BF02473643.

[51] I. Yurtdas, N. Burlion, J.F. Shao, et al., Evolution of the mechanical behaviour of a high performance self-compacting concrete under drying, Cem. Concr. Compos. 33 (2011) 380–388, https://doi.org/10.1016/j.cemconcomp.2010.12.002.

[52] S.N. Shoukry, G.W. William, B. Downie, et al., Effect of moisture and temperature on the mechanical properties of concrete, Constr. Build. Mater. 25 (2011) 688–696, https://doi.org/10.1016/j.conbuildmat.2010.07.020.

[53] W.S. Butcher, The effect of air drying before test: 28-day strength of concrete, Constr. Rev. (1958) 31–32.

[54] A.M. Neville. Properties of Concrete, fourth ed., Pearson Educ. Ltd, London, 2011.